

Supporting Information

A Highly Active Co-Mo-C/NRGO Composite as Efficient Oxygen Electrode for Water-Oxygen Redox Cycle

Chun-Hui Liu,^{a†} Yu-Jia Tang,^{a†} Xiao-Li Wang,^a Wei Huang,^a Shun-Li Li,^{*a} Long-Zhang Dong^a and Ya-Qian Lan^{*a}

^a School of Chemistry and Materials Science, Nanjing Normal University, Nanjing 210023, P. R. China. E-mail: yqlan@njnu.edu.cn.

Experimental Section

Materials. All chemicals were purchased and used without further purification. All solution used in experiments were prepared with Millipore water (18.25 M Ω). The natural graphite powder was purchased from Aladdin. Potassium permanganate (KMnO₄, $\geq 99\%$), hydrogen peroxide (H₂O₂, 30%), hydrazine hydrate (HCl, 36%), concentrated sulfuric acid (H₂SO₄, 98%) and phosphomolybdic acid (H₃PMo₁₂O₄₀·nH₂O, PMo₁₂) were purchased from Sinopharm Chemical Reagent Co. Ltd. Phosphorus (V) oxide (P₂O₅, $\geq 98.0\%$), potassium persulfate (K₂S₂O₈, $\geq 99.5\%$) were purchased from Shanghai lingfeng Chemical Reagent Co. Ltd. Cobalt(II) nitrate hexahydrate (Co(NO₃)₂·6H₂O, $\geq 99.0\%$) was purchased from Guangdong Guanghua Sci-Tech Co. Ltd. Pyrrole (C₄H₅N, $\geq 98.0\%$) was purchased from Shanghai kefeng Industry & Commerce Co. Ltd. Nafion solution (5 wt%) was purchased from Aldrich. Iridium chloride (IrO₂ 99.9% metal basis, Ir $\geq 84.5\%$) was purchased from Shanghai Macklin Biochemical Co. Ltd.

Experimental Methods.

Synthesis of Co-Mo-C/NRGO-1: The graphene oxide was synthesized through chemical exfoliation of graphite powders using a modified Hummers' method. Phosphomolybdic acid (H₃PMo₁₂O₄₀·nH₂O, PMo₁₂) is a kind of classical Keggin type polyoxometalate with strong redox abilities, which can be dissolved in water to produce the polyoxoanion PMo₁₂O₄₀ⁿ⁻. In a typical synthesis, 25 mg of GO films were dissolved in 25 mL of water by ultrasonic treatment for 30 min to obtain a suspension (1 mg mL⁻¹). Next, 0.13 g Co(NO₃)₂·6H₂O and 0.2 g PMo₁₂ (Co : Mo molar ratio = 1:3) were added into the suspension under ultrasonication, followed by introducing the solution with 80 μ L Py in 15 mL water. The solution was transferred into a 50 mL Teflon-lined stainless steel autoclave maintained at 180 °C for 12 h then cooled to room temperature naturally. The product was obtained by filtration and washing with water at least three times. After drying in vacuum at 60 °C, the black powder (the mass is ca. 0.2 g) was obtained and heated at 800 °C for 3 h at a heating rate of 5 °C

min⁻¹ from the room temperature under N₂ (99.99%) atmosphere in a horizontal tube furnace to prepare the Co-Mo-C/NRGO-1. The mass of the obtained Co-Mo-C/NRGO-1 was ca. 0.15 g.

In control experiments, Co-Mo-C/NRGO-2, Co-Mo-C/NRGO-3 and Co-Mo-C/NRGO-4 were synthesized by identical experimental method except the different adding amounts of Co(NO₃)₂·6H₂O, PMo₁₂ and Py precursors. The sample denoted as Co-Mo-C/NRGO-2 was obtained using 0.13 g Co(NO₃)₂·6H₂O, 0.2 g PMo₁₂ and 40 μL Py as the precursor (Co : Mo molar ratio = 1:3) at 180 °C for 12 h and then carbonized at 800 °C. The sample denoted as Co-Mo-C/NRGO-3 was obtained using 0.13 g Co(NO₃)₂·6H₂O, 0.2 g PMo₁₂ and 160 μL PPy as the precursor (Co : Mo molar ratio = 1:3) at 180 °C for 12 h and then carbonized at 800 °C. The sample denoted as Co-Mo-C/NRGO-4 was obtained using 0.38 g Co(NO₃)₂·6H₂O, 0.2 g PMo₁₂ and 80 μL PPy as the precursor (Co : Mo molar ratio = 1:1) at 180 °C for 12 h and then carbonized at 800 °C.

Synthesis of Mo₂C/Co₆Mo₆C₂/NRGO: The as-synthesized Co-Mo-C/NRGO-1 was dispersed in 5 M HCl solution and stirred for 24 h to remove metallic cobalt to obtain Mo₂C/ Co₆Mo₆C₂/NRGO composite.

Synthesis of Mo₂C/NRGO: The Mo₂C/NRGO was synthesized via the method which is similar to the Co-Mo-C/NRGO-1 without adding Co(NO₃)₂·6H₂O.

Synthesis of Co-Mo-C/NRGO-1 with different GO loadings and temperatures: In this article, the amounts of GO were selected as 0 mg, 25 mg (1mg mL⁻¹) and 40 mg (1.6 mg mL⁻¹) to prepare Co-Mo-C/NRGO-1. The Co-Mo-C/NRGO-1 was also obtained by the different carbonization temperatures (700 °C, 800 °C and 900 °C).

Characterization. Powder X-Ray diffraction (PXRD) patterns were recorded on a D/max 2500VL/PC diffractometer (Japan) equipped with graphite monochromatized Cu Kα radiation (λ= 1.54060 Å). Corresponding work voltage and current is 40kV

and 100mA, respectively. Transmission electron microscopy (TEM) was carried out on JEOL-2100F apparatus at an accelerating voltage of 200 kV. High-resolution TEM (HRTEM) image was carried out on FEI Tecnai G2 F30 apparatus at an accelerating voltage of 300 kV. Surface morphologies of the carbon materials were examined by a SEM (JSM-7600F) at an acceleration voltage of 10kV. Elemental mapping and energy dispersive X-ray spectroscopy (EDX) were performed with JSM-5160LV-Vantage typed energy spectrometer. X-ray photoelectron spectroscopy (XPS) was collected on scanning X-ray microprobe (PHI 5000 Versa, ULAC-PHI, Inc.) using Al $\text{K}\alpha$ radiation and the C1s peak at 284.8 eV as internal standard. The Raman spectra of dried samples were obtained on Lab-RAM HR800 with excitation by an argon ion laser (514.5nm). Nitrogen adsorption-desorption isotherms were measured at 77K on a Quantachrome Instruments Autosorb AS-6B. The pore size distributions were measured by the Barrett-Joyner-Halenda (BJH) method.

Electrochemical Measurement. For OER test, electrochemical measurements were performed in a standard three-electrode glass cell on a CHI Instruments 660e electrochemical workstation (Shanghai Chenhua Co. Ltd., China). A glassy carbon electrode (GCE, 3 mm in diameter) was used as the working electrode, Ag/AgCl (in 3 M KCl) as the reference electrode, Pt wire as the counter electrode. The sample was prepared by dispersing 4 mg of catalyst into 2 mL of 9:1 v/v water/Nafion by ultrasonication to form a homogeneous ink. Then 5 μL of the catalyst ink was loaded onto a GCE (loading amount of $\sim 0.14 \text{ mg cm}^{-2}$). Commercial IrO_2 catalyst was also used as a reference sample. 1 M KOH solution was used as the electrolyte and purged with O_2 for 30 min prior to OER test. LSV measurements were conducted with a scan rate of 5 mV s^{-1} . EIS measurements were carried out from 1 000 kHz to 100 mHz with an amplitude of 10mV at the open-circuit voltage. To estimate the electrochemical active surface areas of the catalysts, CV was tested by measuring EDLC under the potential window of 0.2-0.3 V vs. Ag/AgCl with various scan rates (10, 20, 40, 60, 80, and 100 mV s^{-1}). All potentials reported in this paper were converted from vs.

Ag/AgCl to vs. RHE by adding a value of $0.197 + 0.059 \times \text{pH}$. All LSV curves are presented with iR compensation.

For ORR test, a glassy carbon electrode (5 mm in diameter) was used as the working electrode, Ag/AgCl (3 M KCl) as the reference electrode, Pt wire as the counter electrode. Typically, 10 μ L well-dispersed catalysts suspensions were pipetted onto the glassy carbon electrode surface and allowed to dry at room temperature. For comparison, a commercially available Pt/C (20 wt%) catalyst was prepared in the same condition. Cyclic voltammetry experiments were performed from -0.8 to 0.2 V vs. Ag/AgCl at a scan rate of 100 mV s⁻¹ in 0.1 M KOH solutions purged with N₂ or O₂ for at least 30 minutes before testing.

In the rotating disk electrode (RDE) tests, the LSV curves were measured in O₂ saturated 0.1 M KOH solution and the potential was varied from -0.8 to 0.2 V vs. Ag/AgCl with a scan rate of 5 mV s⁻¹ at various rotating speeds from 400 to 1600 rpm.

To examine the ORR performance, the electron transfer number (n) was conducted according to Koutecky-Levich (K-L) equation.

$$(1) j^{-1} = j_L^{-1} + j_k^{-1} = (B\omega^{1/2})^{-1} + j_k^{-1}$$

$$(2) B = 0.62nFC_{O_2}(D_{O_2})^{2/3}\nu^{-1/6}$$

$$(3) j_k = nFkC_{O_2}$$

Where j is the measured current density, j_k and j_L are the kinetic and diffusion-limiting current density, respectively. B is Levich slope which is given by (2). n is the number of electrons transferred for ORR. ω is the rotation rate ($\omega = 2\pi N$, N is the linear rotation speed), F is the Faraday constant ($F = 96485 \text{ C mol}^{-1}$), ν is the kinetic viscosity, and C_{O_2} is the concentration of O₂ ($1.2 \times 10^{-3} \text{ mol L}^{-1}$), and D_{O_2} is the diffusion coefficient of O₂ in 0.1 M KOH ($1.9 \times 10^{-5} \text{ cm}^2 \text{ s}^{-1}$).

Supporting Figures

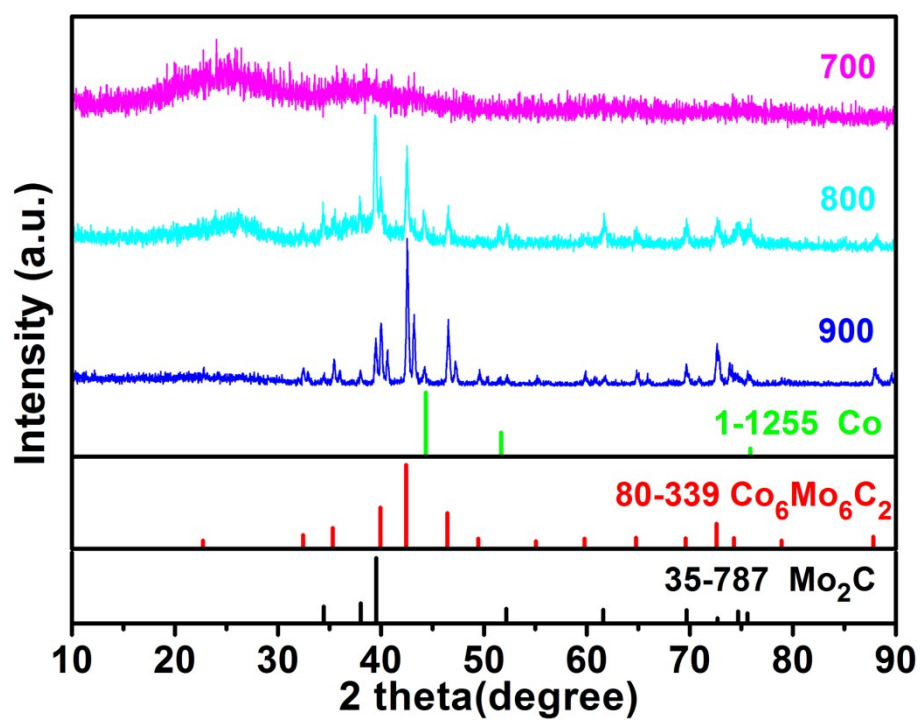


Figure S1. PXRD patterns of Co-Mo-C/NRGO-1 composites carbonized at different temperatures (700 ~ 900°C).

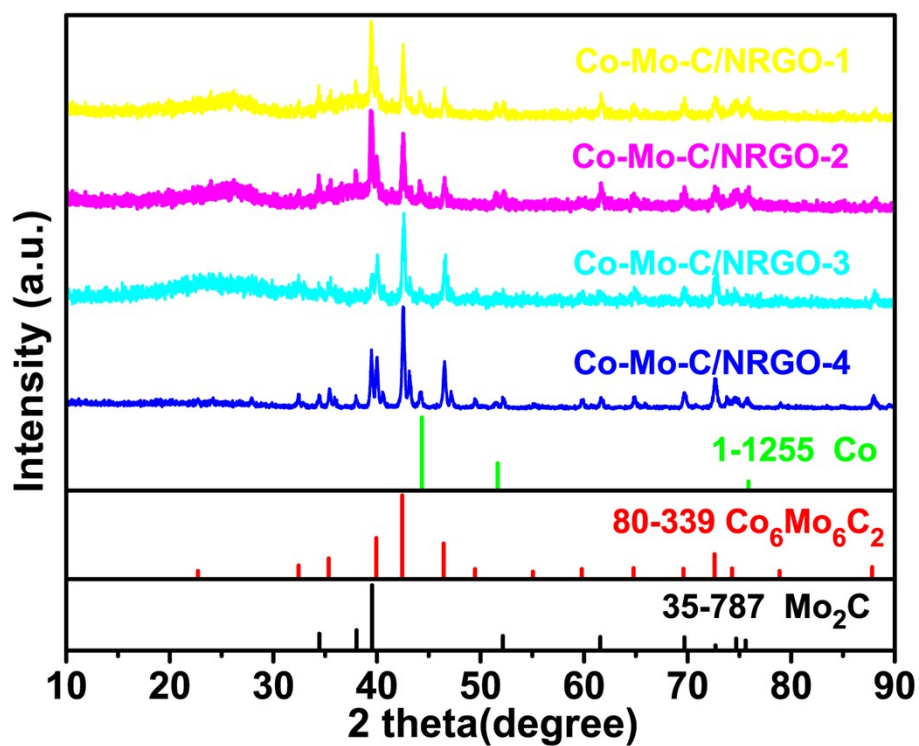


Figure S2. PXRD patterns of Co-Mo-C/NRGO-n (n=1~4) composites with different precursors of PMo₁₂, PPy and Co(NO₃)₂.

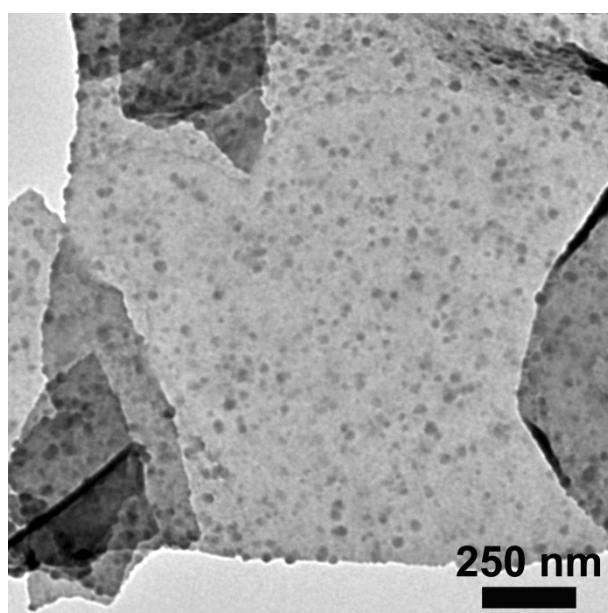


Figure S3. TEM image of Co-PCG composite.

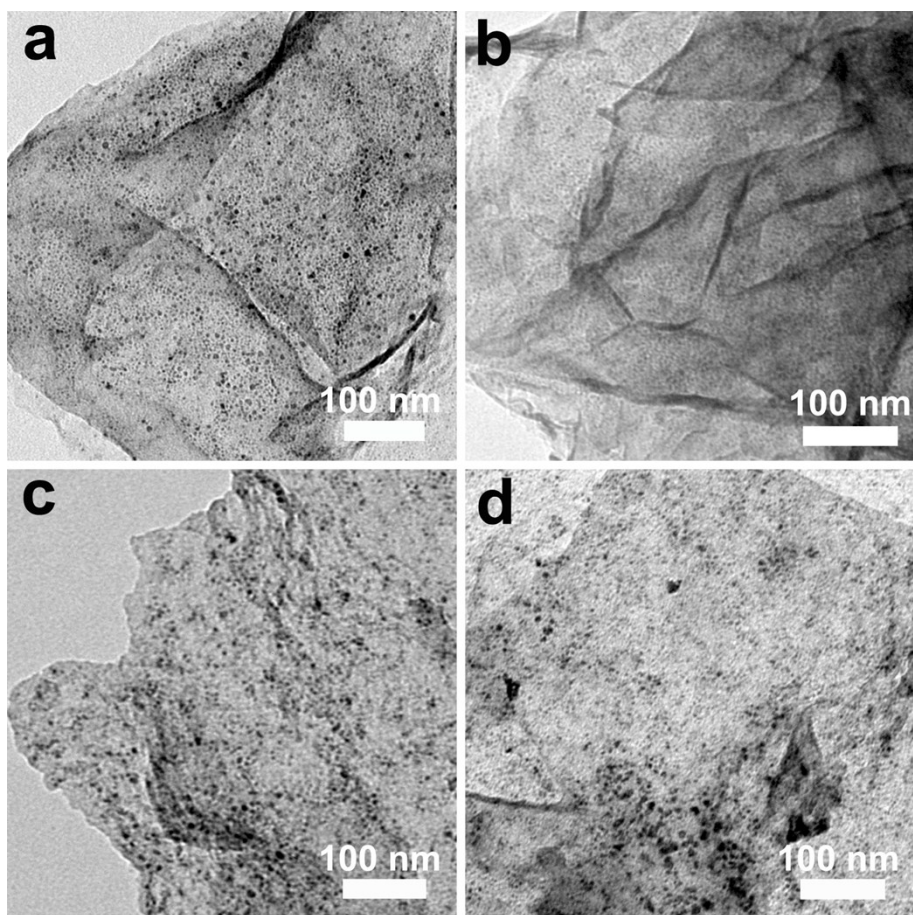


Figure S4. TEM images of (a) Co-Mo-C/NRGO-1, (b) Co-Mo-C/NRGO-2, (c) Co-Mo-C/NRGO-3 and (d) Co-Mo-C/NRGO-4.

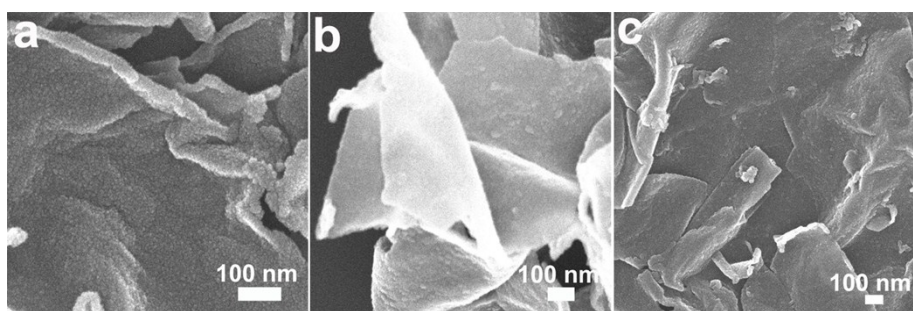


Figure S5. SEM images of (a) Co-Mo-C/NRGO-2, (b) Co-Mo-C/NRGO-3 and (c) Co-Mo-C/NRGO-4.

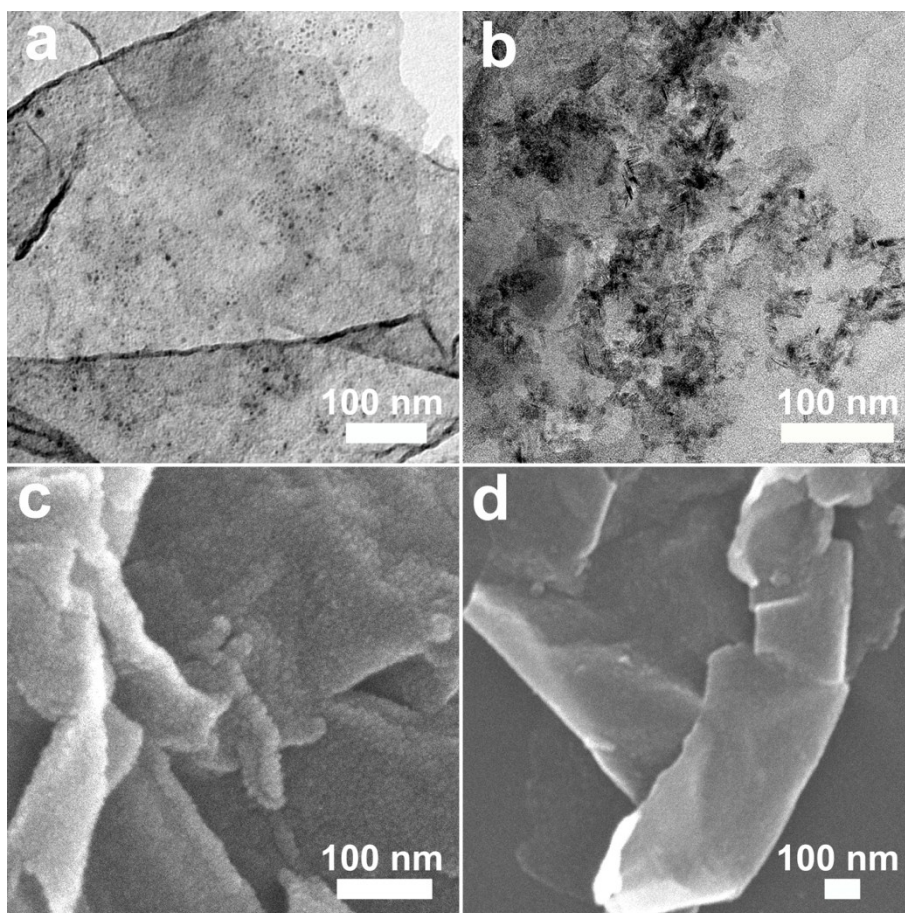


Figure S6. TEM images (a) Mo₂C/Co₆Mo₆C₂/NRGO, (b) Mo₂C/NRGO. SEM images of (c) Mo₂C/Co₆Mo₆C₂/NRGO, (d) Mo₂C/NRGO.

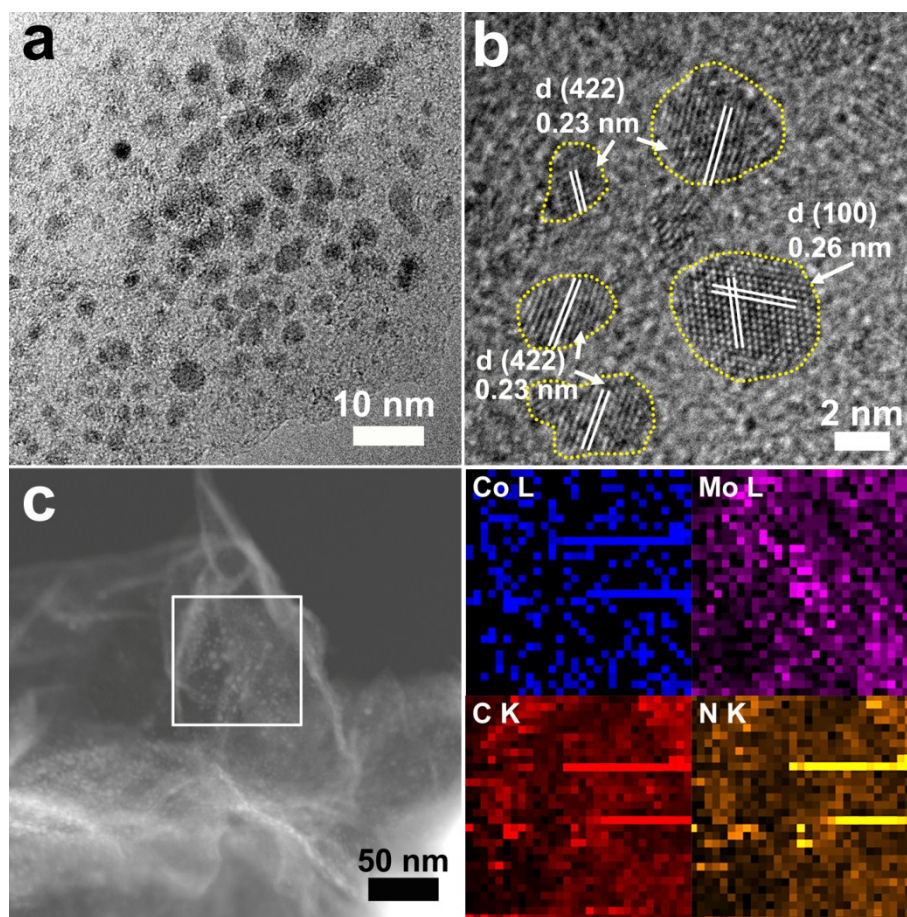


Figure S7. (a) Magnified TEM image of $\text{Mo}_2\text{C}/\text{Co}_6\text{Mo}_6\text{C}_2/\text{NRGO}$ composite. (b) HRTEM image of $\text{Mo}_2\text{C}/\text{Co}_6\text{Mo}_6\text{C}_2/\text{NRGO}$ composite. (c) HAADF-STEM image of $\text{Mo}_2\text{C}/\text{Co}_6\text{Mo}_6\text{C}_2/\text{NRGO}$ and the corresponding EDS mapping of Co, Mo, C and N elements, respectively.

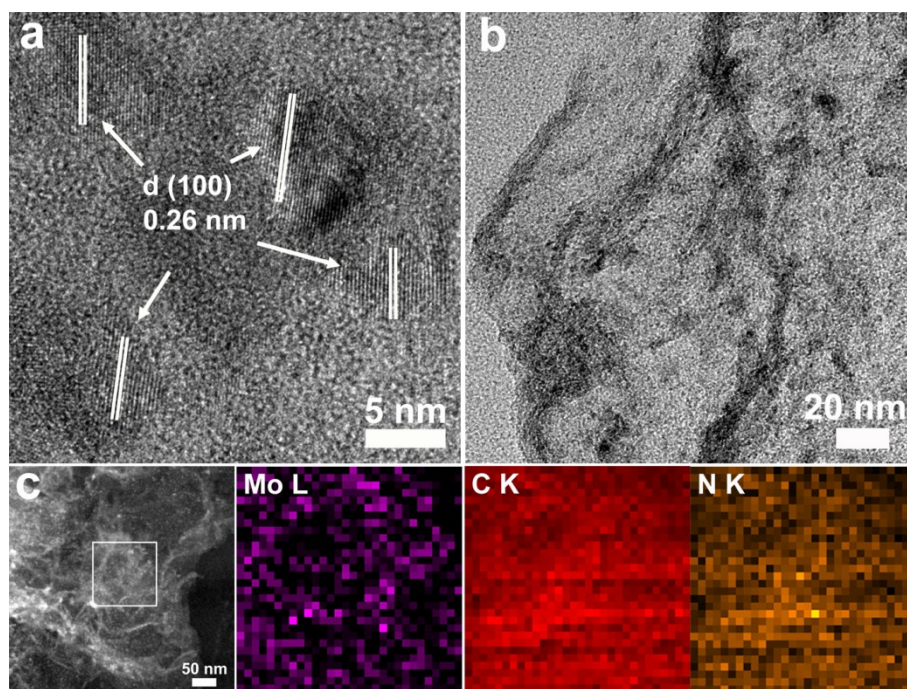


Figure S8. (a) HRTEM image of Mo₂C/NRGO composite. (b) Magnified TEM image of Mo₂C/NRGO composite. (c) HAADF-STEM image of Mo₂C/NRGO and the corresponding EDS mapping of Mo, C and N elements, respectively.

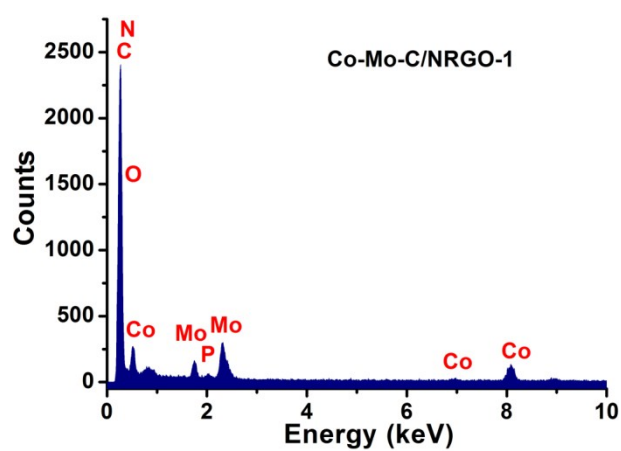


Figure S9. EDX spectrum of Co-Mo-C/NRGO-1 composite.

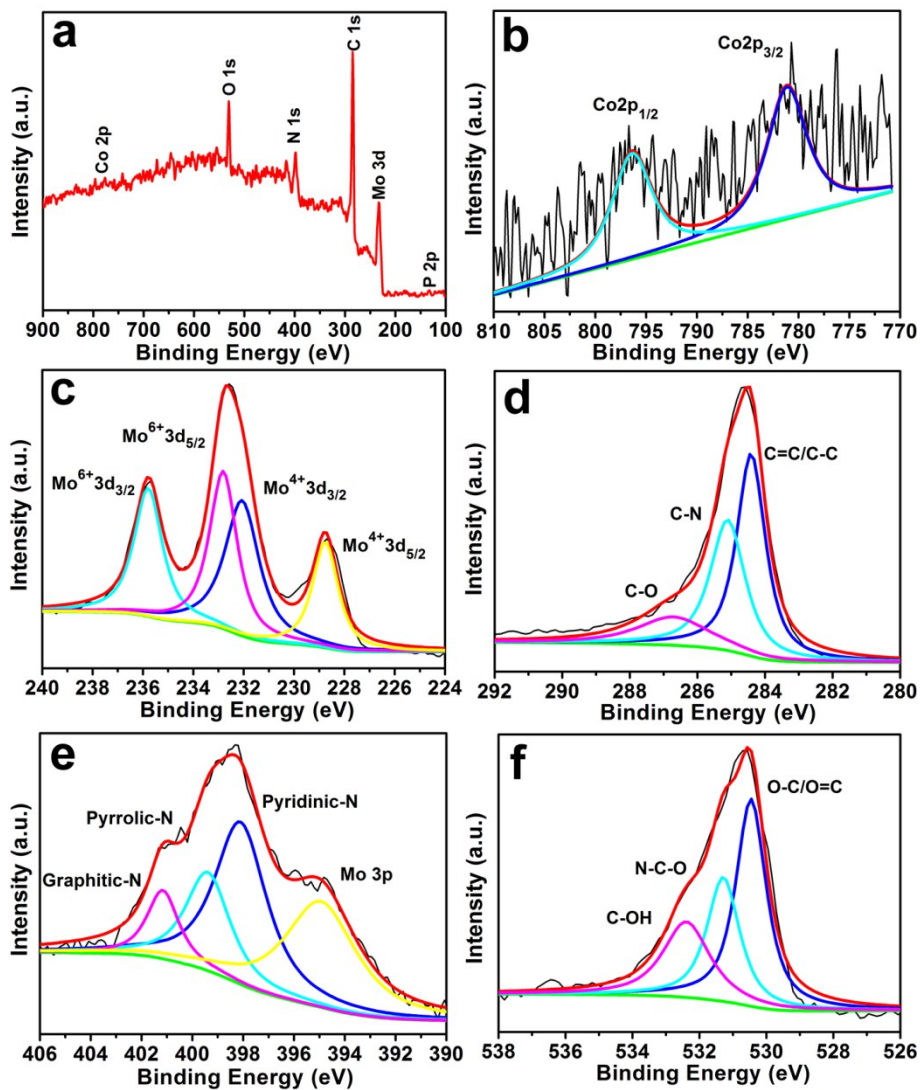


Figure S10. XPS spectrum of Mo₂C/Co₆Mo₆C₂/NRGO composite. (b) Co2p, (c) Mo3d, (d) C1s, (e) N1s and (f) O1s high-resolution XPS spectra.

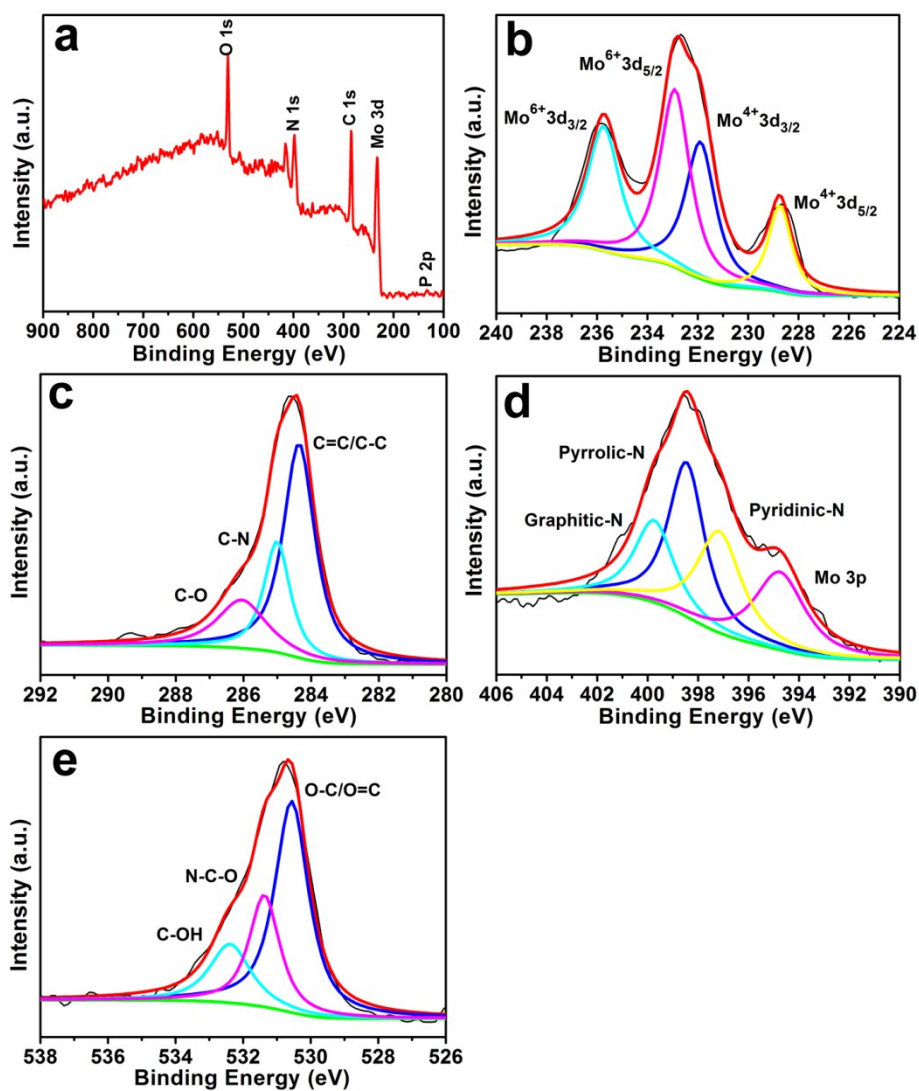


Figure S11. XPS spectrum of Mo₂C/NRGO composite. (b) Mo3d, (c) C1s, (d) N1s and (e) O1s high-resolution XPS spectra.

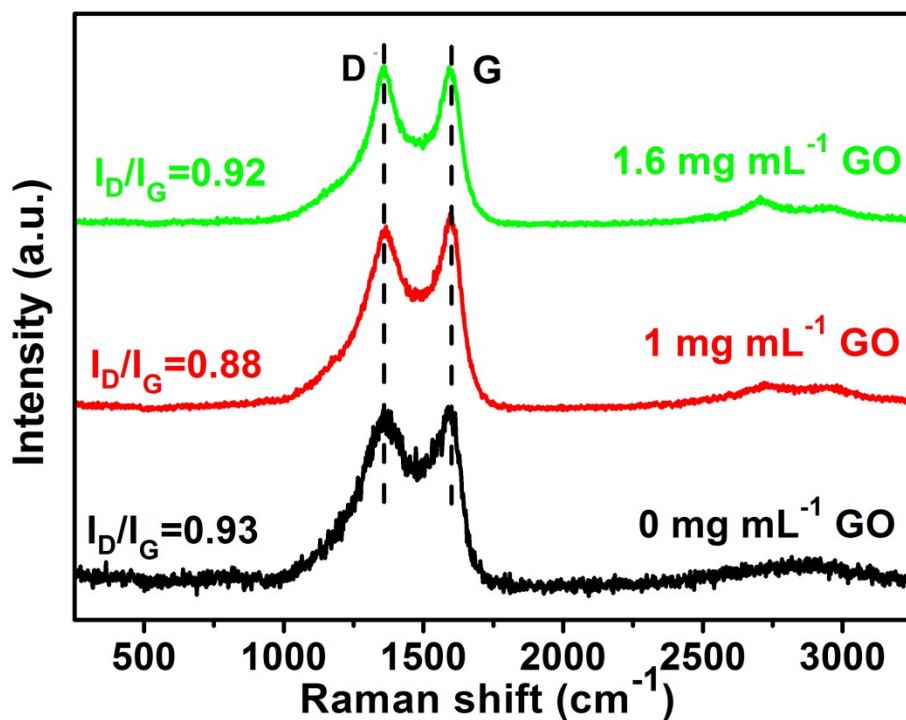


Figure S12. Raman spectrum of Co-Mo-C/NRGO-1 composites with different GO loadings.

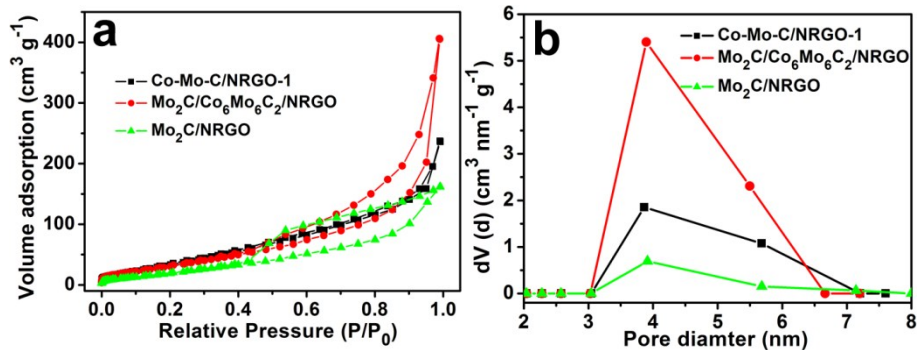


Figure S13. (a) Nitrogen adsorption-desorption isotherms of Co-Mo-C/NRGO-1, Mo₂C/Co₆Mo₆C₂/NRGO, Mo₂C/NRGO. (b) The pore size distribution of the above samples by BJH method.

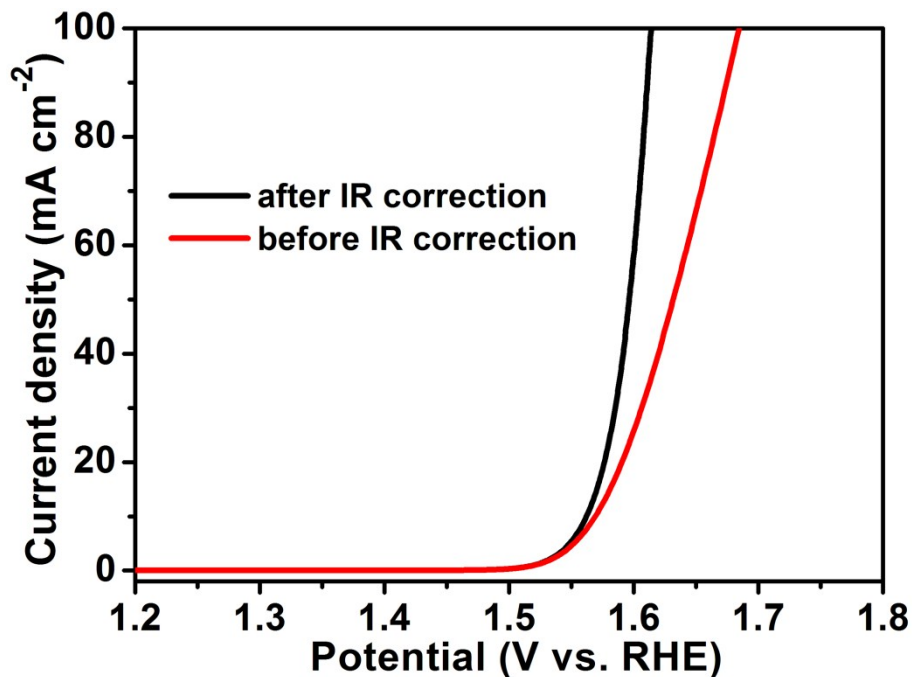


Figure S14. LSV curves of Co-Mo-C/NRGO-1 catalyst before and after iR_s correction.

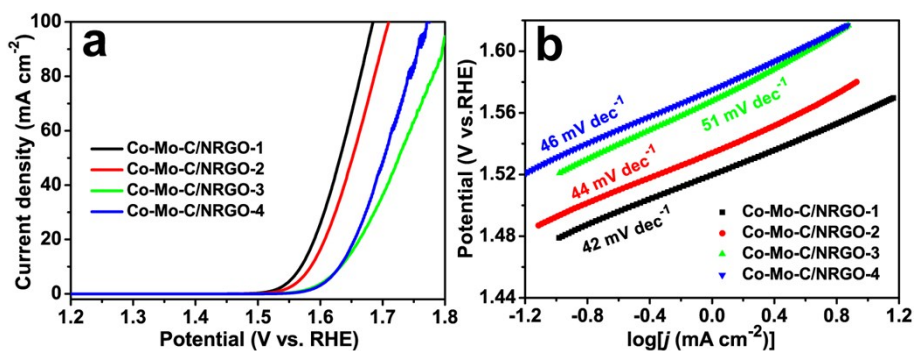


Figure S15. (a) LSV curves for Co-Mo-C/NRGO- n ($n=1\sim 4$) composites prepared with different precursors. (b) The corresponding Tafel plots.

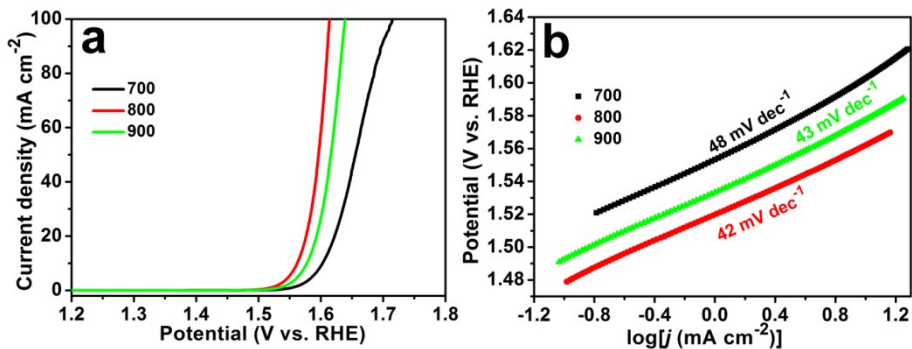


Figure S16. (a) LSV curves for Co-Mo-C/NRGO-1 composites prepared at different carbonization temperatures (700~900 °C). (b) The corresponding Tafel plots.

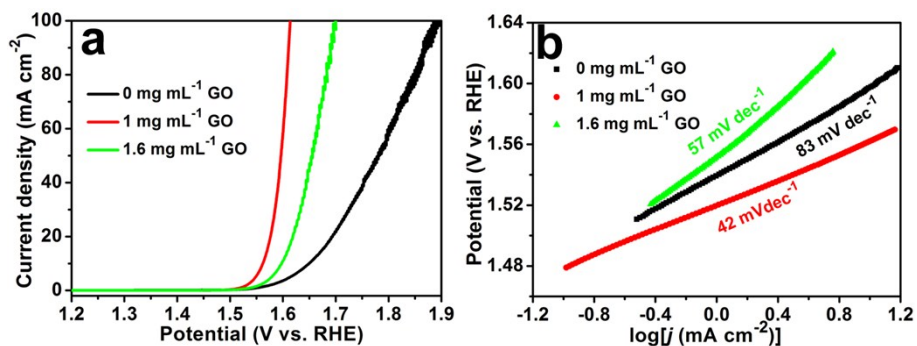


Figure S17. (a) LSV curves for Co-Mo-C/NRGO-1 (n=1~4) composites prepared with different GO loadings. (b) The corresponding Tafel plots.

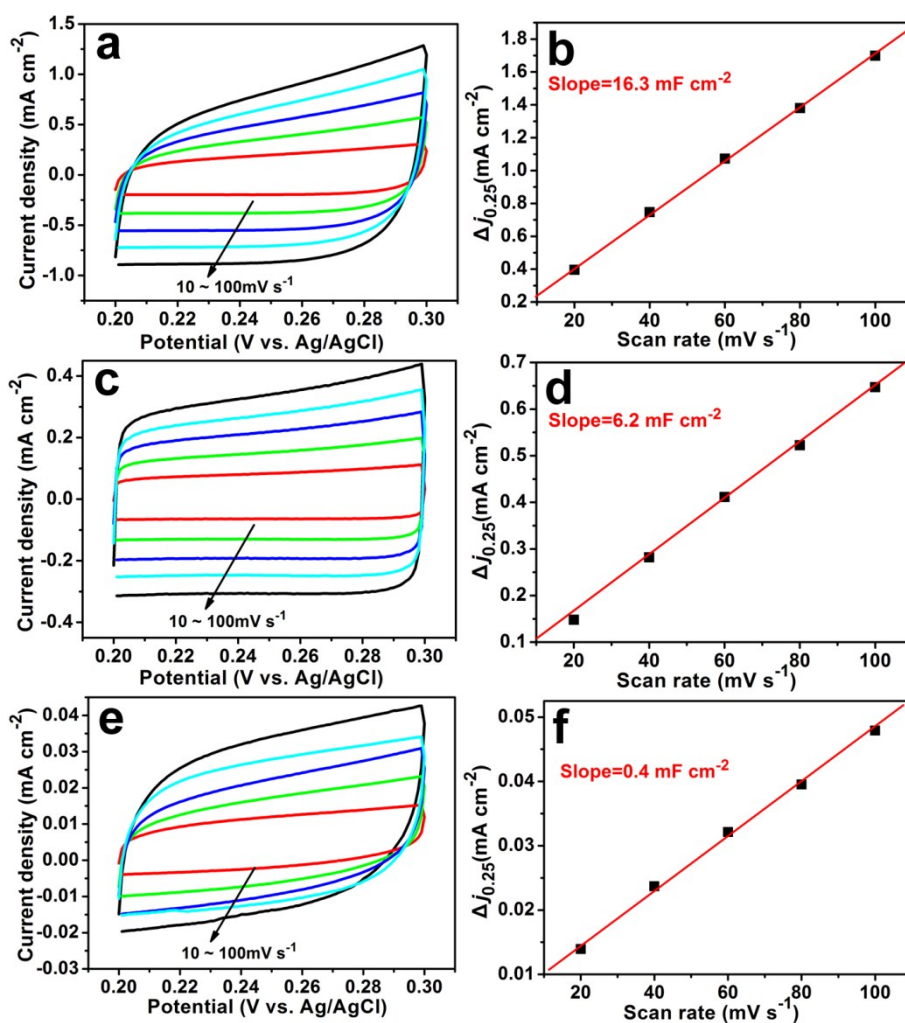


Figure S18. (a, c, e) CV curves for Co-Mo-C/NRGO-1, Mo₂C/Co₆Mo₆C₂/NRGO and Mo₂C/NRGO, respectively at the scan rates from 10 to 100 mV s⁻¹. (b, d, f) The capacitive currents at 0.25 V vs. Ag/AgCl for the corresponding catalysts.

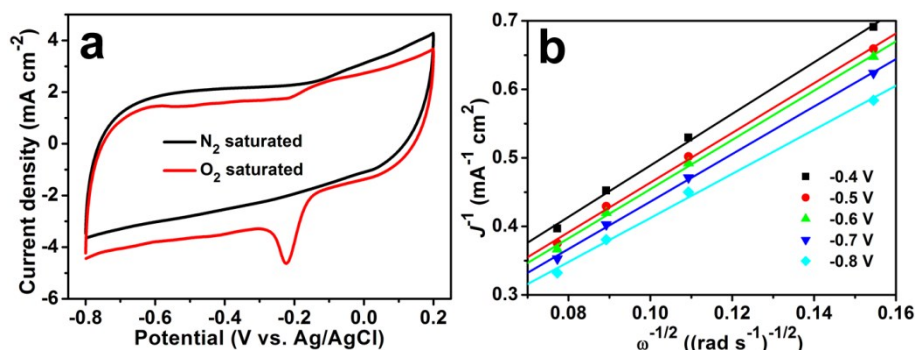


Figure S19. (a) CV curves of Co-Mo-C/NRGO-1 composite in N₂- and O₂-saturated 0.1 M KOH. (b) Kouteck-Levich plots of Co-Mo-C/NRGO-1 composite derived from RDE data.

Table S1. The Co and Mo contents in different catalysts by ICP analysis.

Sample	Co (at.%)	Mo (at.%)
Co-Mo-C/NRGO-1	10.0	45.0
Co-Mo-C/NRGO-2	8.7	38.9
Co-Mo-C/NRGO-3	7.0	27.3
Co-Mo-C/NRGO-4	19.0	45.6

Table S2. Atomic percents of different nitrogen species for different catalysts from XPS analysis.

N species	Co-Mo-C/NRGO-1	Mo ₂ C/Co ₆ Mo ₆ C ₂ /NRGO	Mo ₂ C/NRGO
	Atomic percents (100 %)		
Pyridinic	49.8	56.3	34.0
Pyrrolic	37.8	29.2	41.9
Graphitic	12.4	14.5	24.1

Table S3. Comparison of OER performance in alkaline media for catalysts at this work and some other recently reported Co-based catalysts.

Catalysts	Electrolyte	Substrate	Loading mass (mg cm ⁻²)	η_{10} (mV) ^a	Tafel slope (mV dec ⁻¹)	Reference
Co-Mo-C/NRGO-1	1 M KOH	Glassy carbon	0.14	330	42	This work
np-(Co _{0.52} Fe _{0.48}) ₂ P	1 M KOH	Free-standing	/	270	30	1
CoMn LDH	1 M KOH	Glassy carbon	0.142	324	43	2
Co ₂ B-500	0.1 M KOH	Glassy carbon	0.21	380	45.0	3
Co-P	1 M KOH	Glassy carbon	/	345	47	4
LT-LiCoO ₂	0.1 M KOH	Glassy carbon	0.25	/	52	5
CoMnP	0.1 M KOH	Glassy carbon	0.284	330	61	6
PCPTF	1 M KOH	Glass slide	/	~300	65	7
Co ₃ O ₄ /N-rmGO	1 M KOH	Ni foam	0.24	310	67	8
Co-N-1min	1 M KOH	Nickel foam	1.5	290	70	9
CP/CTs/Co-S	1 M KOH	Carbon paper	~0.32	306	72	10
(Co-NMC) ₁ /NC	0.1 M KOH	Glassy carbon	~0.4	360	83.3	11
CoO _x @CN	1 M KOH	Glassy carbon	~0.12	260	/	12
Co@Co ₃ O ₄ /NC	0.1 M KOH	Glassy carbon	0.21	410	/	13

^a the overpotential at 10 mA cm⁻² reported with respect to RHE and compared with the standard reaction potential of 1.23 V.

Reference.

- [1] Y. Tan, H. Wang, P. Liu, Y. Shen, C. Cheng, A. Hirata, T. Fujita, Z. Tang, M. Chen, *Energy Environ. Sci.* **2016**, *18*, 427.
- [2] F. Song, X. Hu, *J. Am. Chem. Soc.* **2014**, *136*, 16481.
- [3] J. Masa, P. Weide, D. Peeters, I. Sinev, W. Xia, Z. Sun, C. Somsen, M. Muhler, W. Schuhmann, *Adv. Energy Mater.* **2016**, *6*, 1502313.
- [4] N. Jiang, B. You, M. Sheng, Y. Sun, *Angew. Chem. Int. Ed.* **2015**, *54*, 6251.
- [5] T. Maiyalagan, K. A. Jarvis, S. Therese, P. J. Ferreira, A. Manthiram, *Nat.*

Commun. **2014**, *5*, 3949.

[6] D. Li, H. Baydoun, C. N. Verani, S. L. Brock, *J. Am. Chem. Soc.* **2016**, *138*, 4006.

[7] Y. Yang, H. Fei, G. Ruan, J. M. Tour, *Adv. Mater.* **2015**, *27*, 3175.

[8] Y. Liang, Y. Li, H. Wang, J. Zhou, J. Wang, T. Regier, H. Dai, *Nat. Mater.* **2011**, *10*, 780.

[9] Y. Zhang, B. Ouyang, J. Xu, G. Jia, S. Chen, R. S. Rawat, H. J. Fan, *Angew. Chem. Int. Ed.* **2016**, *55*, 8670.

[10] J. Wang, H.-x. Zhong, Z.-l. Wang, F.-l. Meng, X.-b. Zhang, *ACS Nano* **2016**, *10*, 2342.

[11] B. Bayatsarmadi, Y. Zheng, Y. Tang, M. Jaroniec, S.-Z. Qiao, *Small* **2016**, *12*, 3703.

[12] H. Jin, J. Wang, D. Su, Z. Wei, Z. Pang, Y. Wang, *J. Am. Chem. Soc.* **2015**, *137*, 2688.

[13] A. Aijaz, J. Masa, C. Rösler, W. Xia, P. Weide, A. J. R. Botz, R. A. Fischer, W. Schuhmann, M. Muhler, *Angew. Chem. Int. Ed.* **2016**, *55*, 4087.